Quantum information sharing between topologically distinct platforms

Chang-Yu Hou,[1,2] Gil Refael,[1,3] and Kirill Shtengel[2,3,4]
[1]*Department of Physics, California Institute of Technology, Pasadena, California 91125, USA*
[2]*Department of Physics and Astronomy, University of California at Riverside, Riverside, California 92521, USA*
[3]*Institute for Quantum Information and Matter, California Institute of Technology, Pasadena, California 91125, USA*
[4]*Institute for Solid State Physics, University of Tokyo, Kashiwa 277-8581, Japan*
(Received 23 March 2016; revised manuscript received 12 September 2016; published 5 December 2016)

Can topological quantum entanglement between anyons in one topological medium "stray" into a different, topologically distinct medium? In other words, can quantum information encoded nonlocally in the combined state of non-Abelian anyons be shared between two distinct topological media? For one-dimensional topological superconductors with Majorana bound states at the end of system, the quantum information store in those Majorana bound states can be transfered by directly coupling nearby Majorana bound states. However, coupling of two one-dimensional Majorana states will produce a gap, indicating that distinct topological regions of one-dimensional wires unite into a single topological region through the information transfer process. In this paper, we consider a setup with two two-dimensional p-wave superconductors of opposite chirality adjacent to each other. Even two comoving chiral modes at the domain wall between them cannot be gapped through interactions; we demonstrate that information encoded in the fermionic parity of two Majorana zero modes, originally within the same superconducting domain, can be shared between the domains or moved entirely from one domain to another provided that vortices can tunnel between them in a controlled fashion.

DOI: 10.1103/PhysRevB.94.235113

I. INTRODUCTION

The emergence of quasiparticles known as anyons, i.e., particles whose quantum exchange statistics is neither bosonic nor fermionic [1–3], is one of the most interesting collective phenomena in condensed matter systems [4]. An even more exotic possibility opens whenever a multidimensional degenerate Hilbert space is associated with several quasiparticles at fixed positions—these quasiparticles can potentially obey non-Abelian statistics [5–7]. In such a case, braiding of the quasiparticles results in a nontrivial rotation of vector states in this multidimensional subspace. As a consequence, the final state of the system after multiple exchanges depends on their sequence. These properties—the multidimensionality of the Hilbert space combined with the braiding operations which enable transformations of vector states in this space—make non-Abelian anyons a promising platform for quantum computation [7,8]. The nonlocal nature of the computational basis used for encoding quantum information immunizes it from local perturbations; the discreteness of braiding operations promises additional robustness of quantum circuitry that relies on them. Before these conceptual ideas are turned into functioning quantum devices, however, many aspects of topological quantum architecture must be worked out.

One of the important questions from the computational point of view deals with the mechanisms for transferring quantum information between different circuit elements. Ideally, one would imagine that such a transfer happens on-chip between different qubits (or qudits) defined within the same topological medium where braiding and measurement operations are employed to manipulate quantum information. However, this may not always be feasible, particularly if the complexity of quantum devices were to be scaled up. One possible way of transferring quantum information would involve more "conventional," nontopological qubits as intermediate agents [10–14].

An interesting physical question, however, is whether it is possible to transfer quantum information between distinct topological media directly without merging them into one topological phase during the process. An even more interesting question, at least from the physics point of view, is whether such information can be *shared* between two such distinct media. Naively, this seems counterintuitive: topological quantum information is stored in the (superposition of) degenerate states pertaining to a given quantum system; sharing such information would require entanglement between two different quantum systems of macroscopic size. The goal of this paper is to address these questions. As we show, the answer is, surprisingly, affirmative.

One potentially serious obstacle to this idea is that transferring an anyon between two distinct media is not only contingent on an anyon of this type being supported by both media, it also requires that such a transfer is accomplished solely by the means of electron tunneling: fractionalized excitations cannot exist outside of their host media and hence cannot tunnel between them. For example, a fractionally charged Laughlin quasiparticle cannot tunnel between two separate quantum Hall droplets simply due to the fact that each droplet is made of an integral number of electrons. In order to avoid these issues, we focus on a particular example of non-Abelian anyons—Majorana zero modes bound to superconducting vortex cores in chiral p-wave superconductors [15–17]. For more details on Majorana zero modes and their potential utility for topological quantum computation the reader is referred to the recent reviews, Refs. [18] and [19]. While recent experimental advances in detecting Majorana zero modes [20–24] have followed their theoretical predictions in one-dimensional (1D) systems [25–28], in this paper we focus on two-dimensional (2D) systems instead. 2D chiral superconducting systems have a distinct conceptual advantage from our point of view: by considering two superconductors with different chiralities we can be certain that the two topological regions can never be merged

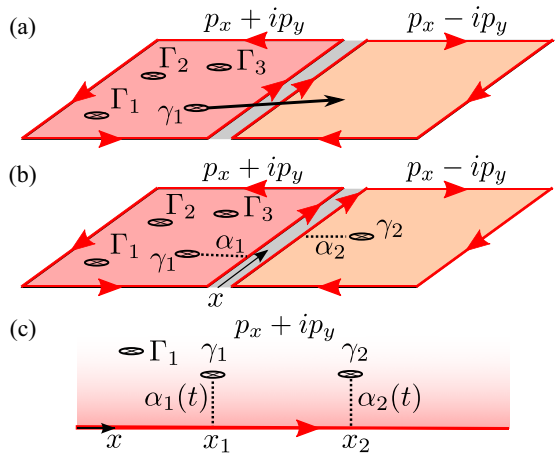

FIG. 1. (a) Idealized setup involving moving a vortex across the domain wall between $p_x + ip_y$ and $p_x - ip_y$ superconductors. Red arrows indicate chiral Majorana edge states at the boundaries of the superconducting domains. γ_1 denotes a Majorana zero mode associated with the vortex being moved, while Γ_1, Γ_2, and Γ_3 represent the stationary modes which, along with γ_1, encode a qubit. (b) The schematic setup of the model we used to "mimic" the move of a vortex across the domain wall. Majorana modes $\Gamma_1, \ldots, \Gamma_3$ are decoupled from the edge states, while γ_1 and γ_2 are coupled to chiral Majorana edge states with time-dependent coupling constants $\alpha_1(t)$ and $\alpha_2(t)$ at $x = x_1$ and $x = x_2$ along the edge, respectively. Here, we assume $x_2 > x_1$. (c) A schematic setup considered in Ref. [9]: two Majorana modes γ_1 and γ_2 coupled to a single chiral Majorana edge with time-dependent coupling constants $\alpha_1(t)$ and $\alpha_2(t)$, respectively.

into one while a Majorana-hosting vortex can be effectively transferred between the two regions. This is in sharp contrast to the case of a 1D topological superconductor, where coupling nearby Majorana bound states to transfer quantum information between two distinct topological regions always opens a gap and effectively merges them into one topological region.

An idealized setup considered in this paper is schematically shown in Fig. 1(a). Quantum information is encoded in the fermionic parity shared between two Majorana zero modes, γ_1, Γ_1. In the standard four-Majorana qubit encoding [29], two additional modes, Γ_2 and Γ_3, serve as a parity reservoir; they do not appear in the mathematical description of our model in any way. The vortices hosting these four Majorana modes are initially located within the same superconducting droplet. One of the vortices is then transferred across the domain wall to a different droplet. Quantum entanglement is maintained if each of the droplets is individually no longer in a state of definitive fermionic parity; instead such parity is a "shared" property of the droplets.

Intuitively, such a transfer should lead to decoherence of quantum information as the domain wall separating the two droplets hosts copropagating gapless chiral edge states [30,31]; these states cannot be gapped and hence even the notion of adiabaticity is not applicable to such a transfer process. However, as we shall see, these gapless edge states can actually be used as intermediate agents facilitating quantum information transfer [32]. We should also mention that in this paper we do not concern ourselves with the actual motion of vortices which host Majorana zero modes. Not only can such a motion lead to other sources of decoherence (e.g., via dissipation in the vortex cores), it is not even obvious what a vortex should look like close to the domain wall between two orthogonal order parameters; supercurrent-carrying Cooper pairs cannot tunnel between the two droplets. We circumvent these issues by considering a simplified model where the locations of all vortices are fixed sufficiently far from the domain wall; instead the couplings of Majorana zero modes to the edge states are varied as functions of time—see Fig. 1(b). When the coupling is weak, the vortex is effectively well-separated from the edge, and when it is large—the vortex essentially becomes a part of the edge [33,34]. By manipulating these couplings, one vortex can be effectively "dissolved" into the edge while another vortex is "nucleated" from the edge on the other side.

The paper is organized as follows. In Sec. II, we present the minimal model describing the low energy degrees of freedom of our Gedanken setup consisting of (i) a pair of coupled copropagating Majorana edge states at the domain wall and (ii) Majorana zero modes hosted inside the droplets and coupled to the edge modes with time-dependent coupling strengths. In Sec. III, we show how this setup allows the quantum information encoded by Majorana zero modes to be transferred across the domain wall. We present analytical results obtained within the Heisenberg picture. In Sec. IV, the amount of transferred quantum information is evaluated within a specific protocol governing the time dependence of the coupling strengths. In Sec. V, we discuss the relevant experimental parameters necessary to achieve high fidelity of such information transfer. Details of derivations are presented in two Appendixes.

II. SETUP

A. Domain wall between $p_x \pm ip_y$ superconductors: Copropagating Majorana edge states

The presence of a pair of copropagating Majorana edge states at a domain wall between $p_x + ip_y$ and $p_x - ip_y$ superconductors, as shown in Fig. 1, is a direct consequence of the fact that $p_x \pm ip_y$ superconductors are in two distinct topological superconducting phases. As both $p_x \pm ip_y$ superconductor are fully gapped in the bulk, these chiral Majorana edge states are the lowest energy degrees of freedom at the domain wall and are described by the Hamiltonian [35]

$$H_e = i \int dx \left\{ -\frac{\hbar v_m}{4} [\eta^L(x)\partial_x \eta^L(x) + \eta^R(x)\partial_x \eta^R(x)] + m(x)\eta^L(x)\eta^R(x) \right\}. \quad (2.1)$$

As shown in Fig. 1(b), $\eta^{L,R}(x)$ are the chiral Majorana edge fields localized at the left and right sides of the domain wall and $m(x)$ is the tunneling coupling strength between two edge fields. The Majorana edge fields obey the anticommutation relation, $\{\eta^i(x), \eta^j(y)\} = 2\delta_{ij}\delta(x - y)$, where $i, j = L, R$. Here, we have assumed that both edge states have the same velocity, v_m. We shall discuss the effect of unequal edge state velocities in Appendix C.

Let us consider Majorana modes localized in the vortex cores as depicted in Fig. 1(b), four of them, $\Gamma_1, \ldots, \Gamma_3$ and γ_1, are on the left side of the domain wall, while the other one, γ_2,

is on the right side. All Majorana operators anticommute with one another and satisfy $\Gamma_a^2 = \gamma_a^2 = 1$. In addition, Majorana operators anticommute with the operators describing the edge fields. Initially, the quantum information (fermion parity) is encoded by two Majorana modes, Γ_1 and γ_1, with eigenvalue $i\Gamma_1\gamma_1(t_0) = \pm 1$ at initial time $t_0 \to -\infty$. Here plus (minus) sign corresponds to odd (even) parity. (As has been pointed out earlier, two additional modes, Γ_2 and Γ_3, serve as a parity reservoir and do not explicitly enter the description of our model). In order to transfer the quantum information, Majorana modes γ_1 and γ_2 are coupled to the chiral Majorana edge field $\eta^L(x_1)$ and $\eta^R(x_2)$, respectively. On the other hand, Γ_a's, the auxiliary Majorana modes needed for encoding the fermionic parity, are decoupled from the edges and from other zero modes. The Hamiltonian governing the dynamics of γ_1 and γ_2 is then

$$H_c = \frac{i}{2}\int dx\{\alpha_1(t)\eta^L(x)\gamma_1\delta(x-x_1) + \alpha_2(t)\eta^R(x)\gamma_2\delta(x-x_2)\}, \tag{2.2}$$

where the coupling strengths $\alpha_a(t)$ for $a \in 1,2$ are time-dependent; by optimizing this time dependence we can control the transfer of quantum information.

As a special consequence of the fact that the 1D chiral modes are copropagating, the coupling between them [whose strength is given by the coupling constant $m(x)$ in Eq. (2.1)] will not induce a gap. Instead, the coupled edge fields can be diagonalized by a spatially dependent unitary transformation

$$\begin{pmatrix}\eta^L(x)\\ \eta^R(x)\end{pmatrix} = \begin{pmatrix}\cos\theta(x) & \sin\theta(x)\\ -\sin\theta(x) & \cos\theta(x)\end{pmatrix}\begin{pmatrix}\eta^1(x)\\ \eta^2(x)\end{pmatrix}, \tag{2.3}$$

where mixing angle θ depends on the coupling between the two edges and is given by

$$\theta(x) = \theta_0 + \int_{x_0}^{x} dx' \frac{2m(x')}{\hbar v_m}. \tag{2.4}$$

In terms of the "rotated fields,", the edge Hamiltonian reads

$$H_e = -\frac{i\hbar v_m}{4}\int dx\,[\eta^1(x)\partial_x\eta^1(x) + \eta^2(x)\partial_x\eta^2(x)], \tag{2.5}$$

while the Hamiltonian describing the coupling of the Majorana zero modes to the edge states becomes

$$H_c = \frac{i}{2}\int dx\left\{\left(\lambda_1^1(t)\eta^1(x)\gamma_1 + \lambda_1^2(t)\eta^2(x)\gamma_1\right)\delta(x-x_1) + \left(\lambda_2^1(t)\eta^1(x)\gamma_2 + \lambda_2^2(t)\eta^2(x)\gamma_2\right)\delta(x-x_2)\right\}. \tag{2.6}$$

Here, coupling constant $\lambda_a^i(t)$ with $i,a \in 1,2$ represents the coupling strength between transformed field $\eta^i(x_a)$ and Majorana zero mode γ_a. The full set of λ_a^i's is given by

$$\begin{aligned}\lambda_1^1(t) &= +\alpha_1(t)\cos\theta(x_1), \quad \lambda_2^1(t) = -\alpha_2(t)\sin\theta(x_2),\\ \lambda_1^2(t) &= +\alpha_1(t)\sin\theta(x_1), \quad \lambda_2^2(t) = +\alpha_2(t)\cos\theta(x_2).\end{aligned} \tag{2.7}$$

When two coupled chiral edge states have different velocities, the low energy effective theory can still be described in terms of two independent chiral edge states [36]. The crucial difference now is that these decoupled Majorana edge states will in general have a nonlinear dispersion, in contrast to the linear dispersion for the case of equal velocities. As a result, there is no simple spatial-dependent unitary transformation, akin to the one given by Eq. (2.3), which decouples the two coupled copropagating edge states. However, as long as the velocity difference difference is small, $\hbar\delta v/m\Delta x \ll 1$ (where $\Delta x = x_2 - x_1$), the essential physics is still captured by the simplified Hamiltonian given by Eq. (2.1), as discussed in Appendix C.

B. Simplified single Majorana edge state setup

The goal of this paper is to analyze the transfer of quantum entanglement between two Majorana zero modes, γ_1 and γ_2, whose dynamics is governed by the Hamiltonian $H = H_e + H_c$ with H_e and H_c given by Eqs. (2.5) and (2.6). In effect, this Hamiltonian describes two zero modes simultaneously coupled to two independent chiral edge states. Prior to delving into this problem, however, let us first study a simplified setup with both Majorana zero modes coupled to a *single* chiral Majorana edge state as shown in Fig. 1(c). The Hamiltonian relevant to this setting is given by

$$H_{SE} = \frac{i}{2}\int dx\left\{-\frac{\hbar v_m}{2}\eta(x)\partial_x\eta(x) + \alpha_1(t)\eta(x)\gamma_1\delta(x-x_1) + \alpha_2(t)\eta(x)\gamma_2\delta(x-x_2)\right\}, \tag{2.8}$$

where we assume $x_2 > x_1$. As shown in Fig. 1(c), we also consider an auxiliary Majorana zero mode, Γ_1 which allows us to define the initial fermion parity, $i\Gamma_1\gamma_1 = \pm 1$. Throughout the whole process, Γ_1 remains decoupled from the edge state and other zero modes and hence does not enter the Hamiltonian (2.8) which governs the dynamics of the system. As in the case of two edge states, here the time-dependent coupling strengths α_a control the transfer of quantum information. We note that employing a chiral edge state of a topological medium to transport quantum information has been previously discussed in a different context in Ref. [32].

In what follows, we first study this simplified setup and establish the necessary formalism to investigate how the quantum information stored in the Majorana mode γ_1 can be transferred to the Majorana mode γ_2. We will then apply this formalism to study the original setup described by Hamiltonian Eqs. (2.1) and (2.2) and discuss the relation of the original setup and the simplified setup.

III. TRANSFERRING QUANTUM INFORMATION

A. Single Majorana edge state

A straightforward way to understand the time evolution of quantum states is to employ the Heisenberg picture in quantum mechanics. From Eq. (2.8) together with the commutation relations, the Heisenberg equations of motion of operators are given by

$$(\partial_t + v_m\partial_x)\eta = \frac{\alpha_1}{\hbar}\gamma_1\delta(x-x_1) + \frac{\alpha_2}{\hbar}\gamma_2\delta(x-x_2), \tag{3.1a}$$

$$\partial_t\gamma_1(t) = -\frac{\alpha_1(t)}{\hbar}\eta(x_1,t), \tag{3.1b}$$

$$\partial_t\gamma_2(t) = -\frac{\alpha_2(t)}{\hbar}\eta(x_2,t). \tag{3.1c}$$

In terms of the initial operators, $\bar{\gamma}_a \equiv \gamma_a(t_0)$ and $\eta(x,t_0)$, the time evolved operators $\gamma_a(t)$ are given by

$$\gamma_1(t) = K_1(t_0,t)\,\bar{\gamma}_1 - \int_{t_0}^{t} dt'\,\alpha_1(t')\,K_1(t',t)\,\eta^{(0)}(x_1,t'), \quad (3.2a)$$

$$\gamma_2(t) = K_2(t_0,t)\,\bar{\gamma}_2 + W(t_0,t,\Delta x)\,\bar{\gamma}_1 - \int_{t_0}^{t} dt'\,\alpha_2(t')\,K_2(t',t)\,\eta^{(1)}(x_2,t'). \quad (3.2b)$$

Note that Eq. (3.2a) contains $\eta^{(0)}(x,t) \equiv \eta(x - v_m(t - t_0),t_0)$, an unperturbed chiral Majorana edge field. On the other hand, Eq. (3.2b) contains $\eta^{(1)}(x,t)$—an edge field already perturbed by the "upstream" coupling with γ_1. The evolution of the edge field $\eta^{(1)}(x_2,t)$ is given by

$$\eta^{(1)}(x_2,t) = \eta^{(0)}(x,t) - \Theta\left(t - \left(t_0 + \frac{\Delta x}{v_m}\right)\right)\frac{\alpha_1(t - \Delta x/v_m)}{\hbar^2 v_m} \times \int_{t_0}^{t-\frac{\Delta x}{v_m}} d\tau_0\,\alpha_1(\tau_0)\,K_1(\tau_0,t-\Delta x/v_m)\,\eta^{(0)}(x_1,\tau_0). \quad (3.3)$$

A detailed derivation of Eqs. (3.2) and (3.3) is presented in Appendix A. The two functions which determine the time evolution of operators in Eqs. (3.2) and (3.3) are the kernel function

$$K_a(t_i,t_f) = \exp\left[-\int_{t_i}^{t_f} \frac{\alpha_a(t')^2}{2\hbar^2 v_m} dt'\right], \quad (3.4)$$

and the weight function

$$W(t_0,t,\Delta x) = -\int_{t_0+\frac{\Delta x}{v_m}}^{t} dt'\,\frac{\alpha_2(t')\,\alpha_1(t' - \Delta x/v_m)}{\hbar^2 v_m} \times K_2(t',t)\,K_1(t_0,t' - \Delta x/v_m). \quad (3.5)$$

Several comments are in order. First, $\gamma_a(t)$ as well as $\eta(x,t)$ satisfy the proper equal-time anticommutation relations, as should be expected from unitarity. The first terms in Eqs. (3.2a) and (3.2b) represent the loss of memory of the initial conditions for both operators to the coupling of the corresponding zero modes to the edge. Most importantly, the second term in Eq. (3.2b) describes how the second Majorana mode $\gamma_2(t)$ acquires the memory of the initial condition for $\gamma_1(0)$; the weight function $W(t_0,t,\Delta x)$ given by Eq. (3.5) is exactly the quantum information transferred from the zero mode $\bar{\gamma}_1$ to $\gamma_2(t)$. Explicitly, let us consider the case where the operator $i\Gamma_1\gamma_1(t_0)$ has eigenvalue ± 1 for the initial quantum state. Using Eq. (3.2b), we have $\langle i\Gamma_1\gamma_2(t)\rangle = \pm W(t_0,t,\Delta x)$, which represents the fidelity of the quantum information transfer. In the next section, we will show that owing to the chiral nature of the edge state, a high fidelity of transfer can be achieved by employing specific protocols for $\alpha_a(t)$.

As a side note, a nonzero expectation value of $\langle i\gamma_1\gamma_2(t)\rangle$ will also develop. Physically, this phenomenon comes from the edge-state coupling that correlates two Majorana zero modes and can be understood as contributions from the $\eta^{(0,1)}(x,t)$ terms in Eqs. (3.2). This polarization reaches its peak value of $2/\pi$ in the limit of $\Delta x \to 0$ with the time-independent couplings of equal strength, $\alpha_1 = \alpha_2$ [9,34]. Our approach provides a clear interpretation for the origin of this polarization, which is discussed in more detail in Appendix B.

B. Two copropagating Majorana edge states

Having analyzed the case of single edge coupling, we are now ready to discuss the actual setup of interest shown in Fig. 1(b) where two Majorana modes are coupled to two copropagating chiral Majorana edge states, respectively. The strategy remains the same: starting with the Hamiltonian given by Eqs. (2.5) and (2.6), to solve the Heisenberg equation of motion, akin to Eq. (3.1), and to obtain the time evolution of Majorana modes $\gamma_a(t)$ in the following form:

$$\gamma_1(t) = K_1(t_0,t)\bar{\gamma}_1 + \cdots,$$
$$\gamma_2(t) = K_2(t_0,t)\bar{\gamma}_2 + W_{2E}(t_0,t,\Delta x)\bar{\gamma}_1 + \cdots. \quad (3.6)$$

Here, the $\cdots$ represents contributions from $\eta^{L,R}(x,t_0)$. As those terms play no part in the quantities we are interested in, we will omit them for simplicity. Again, $\bar{\gamma}_a \equiv \gamma_a(t_0)$ represent initial operators while the kernel function K_a is defined in Eq. (3.4).

The weight function, which describes the transfer of the quantum entanglement across the domain wall, can be related to that of the single Majorana edge state in Eq. (3.5) by

$$W_{2E}(t_0,t,\Delta x) = W(t_0,t,\Delta x)\sin\Delta\theta. \quad (3.7)$$

The phase factor $\Delta\theta$ depends on the coupling strength $m(x)$ between two chiral Majorana edge states and is given by

$$\Delta\theta = -\int_{x_1}^{x_2} dx'\,\frac{2m(x')}{\hbar v_m}. \quad (3.8)$$

The reduction of the fidelity for quantum information transfer due to this phase factor can be intuitively understood as follows. The coupling $m(x)$ between two Majorana edge states spatially interchanges contents of the edge fields $\eta^{L,R}(x)$ in terms of the mixed edge fields $\eta^{1,2}(x)$. As a result, the quantum entanglement associated with the initial operator $\bar{\gamma}_1$ carried away by the edge field $\eta^L(x)$ from $x = x_1$ is partially transferred across the domain wall with the ratio $\sin\Delta\theta$ and is then picked up by the γ_2 coupled to the edge field $\eta^R(x)$ at $x = x_2$.

IV. TIME-DEPENDENT PROTOCOL AND QUANTUM INFORMATION TRANSFER

To mimic the process of moving a vortex across the domain wall, the time-dependent profiles for coupling strengths $\alpha_a(t)$ are chosen to satisfy the following boundary conditions. At the initial time $t \to -\infty$, Majorana mode γ_1 is decoupled from the edge while Majorana mode γ_2 is strongly coupled to the edge. At the end of the process, $t \to \infty$, the Majorana mode γ_1 is strongly coupled to the edge while the mode γ_2 becomes decoupled from the edge. We choose to parametrize the time dependence of the coupling strengths as

$$\alpha_1(t) = \frac{\Lambda}{2}(1 + \tanh\beta t),$$
$$\alpha_2(t) = \frac{\Lambda}{2}(1 - \tanh\beta(t - \Delta t)), \quad (4.1)$$

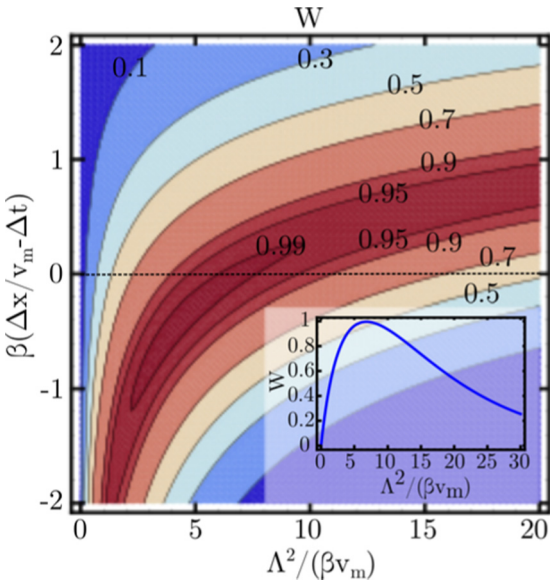

FIG. 2. Contour plot shows the weight $W(t_0,t,\Delta x)$ as a function of dimensionless parameters, $\Lambda^2/\beta\hbar^2 v_m$ and $\beta(\Delta x/v_m - \Delta t)$. The weight function is given in Eq. (3.5) and is evaluated using the time-dependent coupling strengths given in Eq. (4.1). The inset shows the weight function W along the line cut $\beta(\Delta x/v_m - \Delta t) = 0$ as indicated by the dashed horizontal line.

which satisfy the aforementioned boundary conditions. Here, Λ determines the strength of the coupling between the Majorana modes in the bulk and the edge states, the inverse time constant β controls how fast the couplings are turned on and off, and Δt is the time delay between the two processes.

With these time-dependent coupling constants, the weight function $W(t_0,t,\Delta x)$ in Eq. (3.5) is governed by two dimensionless parameters, $\Lambda^2/\beta\hbar^2 v_m$ and $\beta(\Delta x/v_m - \Delta t)$. We evaluate the weight function with time $t \to \infty$ and plot the weight strength as functions of these two dimensionless parameters in Fig. 2. When both Majorana modes couple to single Majorana edge, the quantum information transferred from Majorana mode γ_1 to γ_2 is fully determined by this weight strength. From Fig. 2, one can easily achieve more than 95% of fidelity for quantum information transferring. The inset of Fig. 2 shows the weight function $W(t_0,t\to\infty,\Delta x)$ along the line $\beta(\Delta x/v_m - \Delta t) = 0$. The peak value of this function is about 99.6% and can be achieved by tuning the ratio of $\Lambda^2/(v_m\hbar^2\beta)$. That is, there is a range of parameters allowing for a reasonable amount of quantum information to be transferred across the domain wall.

The fidelity of the information transfer across a chiral p-wave domain wall can be further reduced by the factor $\sin\Delta\theta$—see Eq. (3.7). However, as we discuss in the next section, this problem can be in principle alleviated, resulting in an optimal quantum information transfer.

V. DISCUSSION

Let us now discuss the experimental parameters pertinent to our setup and their tunability for optimizing the transfer of quantum information across the domain wall separating two p-wave superconductors with opposite chiralities. To reach the optimal fidelity, the accumulated phase in Eq. (3.8) due to the coupling between chiral Majorana edge states has to be $\Delta\theta = \pi/2\ (\mathrm{mod}\pi)$, while the weight function $W(t_0,t\to\infty,\Delta x)$ should be at its maximum.

In order to satisfy the former condition, we observe that the coupling strength $m(x)$ relates to the superconducting phase difference $\Delta\phi(x)$ across the domain wall by $m(x) = m_0(x)\cos(\Delta\phi(x)/2)$ [30,31]. Here $m_0(x)$ is the bare coupling strength along the domain in the absence of the phase difference. As threading a magnetic field through the domain wall effectively changes the phase difference $\Delta\phi(x)/2$, it effectively tunes the coupling strength $m(x)$. Hence the accumulated phase can be adjusted to $\Delta\theta = \pi/2\ (\mathrm{mod}\pi)$. With the estimated value of the bare coupling strength $m_0 \sim 0.025$ meV and the typical edge velocity $v_m \sim 10^5$ m/s [35], the accumulated phase is estimated to be $\Delta\theta \sim \Delta x \times 10^6\ \mu\mathrm{m}^{-1}$. This implies that Δx should be of order 1–2 μm in order to have $\Delta\theta = \pi/2$.

On the other hand, the weight strength $W(t_0,t\to\infty,\Delta)$ can be tuned by β, Λ, and Δt. Assuming that the inverse time constant is in the range of $\beta \sim 10^6$–$10^9\ \mathrm{s}^{-1}$, it should be easy to achieve sufficiently small values of $\beta(\Delta x/v_m - \Delta t)$ when Δx is in the order of 1–2 μm and edge velocity $v_m \sim 10^5$ m/s. With this condition, the weight function reaches its peak value with the ratio $\Lambda^2/(v_m\hbar^2\beta) \sim 7$, as seen in the inset of Fig. 2. This requires the value of $\Lambda \sim 5\times10^{-10}$–$2\times10^{-8}\ \mathrm{eV\,m}^{1/2}$. Again, we should emphasis that the actual values of β and Λ are not essential. Instead, it is their combination, $\Lambda^2/(v_m\hbar^2\beta)$, that is crucial for determining the amount of quantum information transferred.

It is also worth mentioning that while we have studied a specific protocol given by Eq. (4.1), other protocols may lead to even more reliable transfer of quantum entanglement.

VI. CONCLUSION

We have described a process whereby quantum entanglement associated with Majorana zero modes in a chiral p-wave superconductor can stray from the original medium into another, topologically distinct medium. As a result, the topological quantum information initially encoded within one superconducting domain can now be shared between two domains of opposite chirality. In principle, this can be done very efficiently provided that the fermion tunneling between superconducting vortices and edge states can be judiciously controlled. From the physical point of view, this effect can be understood from the fact that the quantum information is encoded in the fermionic parity. Different domains, even though topologically distinct, need not be in the parity eigenstates individually; coupling their respective edge states through fermionic tunneling provides a mechanism for moving this parity across and creating entangled states between the domains. Utilizing this mechanism repeatedly, quantum information can be transferred from one medium to another directly, without any need for measuring it or employing intermediate quantum buses.

The reliance of our proposed setup on fermionic tunneling does appear to be a limiting factor as far as potential generalizations of this scheme to other topological platforms are concerned. Unfortunately, it is not clear to us how this constraint can be physically avoided in the cases of more exotic non-Abelian anyons.

While our idealized setup does not take into account some "real life" complications, such as a finite stretch of the edge state (rather than its single point) coupled to a vortex—which will somewhat degrade the fidelity of the information transfer—our main goal has been to provide a "proof of principle." Further optimization of the transfer protocols with an eye on those experimentally relevant effects should be a subject of future research.

ACKNOWLEDGMENTS

The authors would like to thank D. Clarke and N. Lindner for helpful discussions. C.Y.H. and K.S. were supported in part by the DARPA-QuEST program. K.S. was supported in part by NSF Grant No. DMR-1411359. C.Y.H. and G.R. acknowledge the support from the Packard foundation and NSF Grant No. DMR-1410435. The authors are also grateful to the IQIM, an NSF center supported in part by the Moore foundation. In addition G.R. would like to acknowledge the hospitality of the Aspen Center for Physics where part of the work was done.

APPENDIX A: SOLUTION OF THE EQUATION OF MOTION

Let us recall the Heisenberg equation of motion (EOM) in Eq. (3.1) for the case of single chiral Majorana edge state:

$$(\partial_t + v_m\partial_x)\eta = \frac{\alpha_1}{\hbar}\gamma_1\delta(x-x_1) + \frac{\alpha_2}{\hbar}\gamma_2\delta(x-x_2), \quad \text{(A1a)}$$

$$\partial_t\gamma_1(t) = -\frac{\alpha_1(t)}{\hbar}\eta(x_1,t), \quad \text{(A1b)}$$

$$\partial_t\gamma_2(t) = -\frac{\alpha_2(t)}{\hbar}\eta(x_2,t). \quad \text{(A1c)}$$

Here operators in Eqs. (A1) are in the Heisenberg picture. The goal is to solve these EOM, i.e., how these operators evolute as the function of time given the initial operators, $\bar{\gamma}_a = \gamma_a(t_0)$ and $\bar{\eta}(x,t_0) = \eta(x,t_0)$, at time $t = t_0 \to -\infty$.

To solve these EOMs in Eqs. (3.1), we first observe that the retarded Green functions for $\eta(x,t)$ and $\gamma_a(t)$ are given by

$$G_\eta(x,t;x',t') = \Theta(t-t')\delta(x-x'-v_m(t-t')), \quad \text{(A2a)}$$

$$G_{\gamma_a}(t,t') = \Theta(t-t'), \quad \text{(A2b)}$$

where $\Theta(t)$ is a Heaviside Θ function. We can then relate the $\eta(x,t)$ field with Majorana modes $\gamma_a(t)$ from Eq. (A1a) and give $\eta(x_a,t)$ as

$$\eta(x_1,t) = \Theta(t-t_0)\frac{\alpha_1(t)}{2\hbar v_m}\gamma_1(t), \quad \text{(A3)}$$

$$\eta(x_2,t) = \Theta\left(t-t_0-\frac{\Delta x}{v_m}\right)\frac{\alpha_1(t-\Delta x/v_m)}{\hbar v_m}\gamma_1\left(t-\frac{\Delta x}{v_m}\right) + \frac{\alpha_2(t)}{2\hbar v_m}\Theta(t-t_0)\gamma_2(t), \quad \text{(A4)}$$

where $\Delta x \equiv x_2 - x_1 > 0$ and we have used $\Theta(0) \equiv 1/2$. On the other hand, $\gamma_a(t)$ can be related to $\eta(x_a,t)$ by Eqs. (A1b) and (A1c) as

$$\gamma_a(t) = -\int_{t_0}^{t} dt' \frac{\alpha_a(t')}{\hbar}\eta(x_a,t')dt'. \quad \text{(A5)}$$

We can now obtain a set of coupled differential equations only for Majorana modes by substituting Eqs. (A3) and (A4) into Eqs. (A1b) and (A1b) yielding

$$\partial_t\gamma_1(t) = -\Theta(t-t_0)\frac{\alpha_1(t)^2}{2\hbar^2 v_m}\gamma_1(t), \quad \text{(A6a)}$$

$$\partial_t\gamma_2(t) = -\Theta\left(t-\left(t_0+\frac{\Delta x}{v_m}\right)\right)\frac{\alpha_2(t)\alpha\left(t-\frac{\Delta x}{v_m}\right)}{\hbar^2 v_m}\gamma_1 \times\left(t-\frac{\Delta x}{v_m}\right) - \Theta(t-t_0)\frac{\alpha_2(t)^2}{2\hbar^2 v_m}\gamma_2(t). \quad \text{(A6b)}$$

In terms of initial operators $\gamma_a(t_0) \equiv \bar{\gamma}_a$, solutions of these differential equations give the first part of solution in Eq. (3.2), and $K_a(t_0,t)$ and $W(t_0,t,\Delta x)$ in Eqs. (3.4) and (3.5).

On the other hand, a decoupled integral-differential equation for $\eta(x,t)$ can be obtained similarly and is given by

$$(\partial_t + v_m\partial_x)\eta(x,t) = -\frac{\alpha_1(t)}{\hbar^2}\Theta(t-t_0)\delta(x-x_1)\int_{t_0}^{t} dt'\alpha_1(t')\eta(x_1,t') - \frac{\alpha_2(t)}{\hbar^2}\Theta(t-t_0)\delta(x-x_2)\int_{t_0}^{t} dt'\alpha_2(t')\eta(x_2,t'). \quad \text{(A7)}$$

As $\eta(x,t)$ is a chiral field, we can include the effect of couplings at $x = x_1$ and $x = x_2$ in sequence for solving this integral-differential equation. Therefore, let us consider the first part of the integral-differential equation

$$(\partial_t + v_m\partial_x)\eta^{(1)}(x,t) = -\frac{\alpha_1(t)}{\hbar^2}\Theta(t-t_0)\delta(x-x_1)\int_{t_0}^{t} dt'\alpha_1(t')\eta^{(1)}(x_1,t'), \quad \text{(A8)}$$

which implies the following formal solution:

$$\eta^{(1)}(x,t) = \eta^{(0)}(x,t) - \Theta(x-x_1)\frac{\alpha_1(t-\frac{x-x_1}{v_m})}{\hbar^2 v_m} \times\int_{t_0}^{t-\frac{x-x_1}{v_m}} d\tau\,\alpha_1(\tau)\eta^{(1)}(x,\tau). \quad \text{(A9)}$$

Here, $\eta^{(0)}(x,t) \equiv \eta(x - v_m(t-t_0),t_0)$ originates from the chiral flow of the initial Majorana edge field. Then, the full solution can be solved iteratively and can be formally expressed by

$$\eta^{(1)}(x,t) = \eta^{(0)}(x,t) - \Theta(x-x_1)\frac{\alpha_1(t-\frac{x-x_1}{v_m})}{\hbar v_m}\left\{\int_{t_0}^{t-\frac{x-x_1}{v_m}} d\tau_0\frac{\alpha_1(\tau_0)}{\hbar}\eta^{(0)}(x_1,\tau_0) - \int_{t_0}^{t-\frac{x-x_1}{v_m}} d\tau_0\frac{\alpha_1(\tau_0)^2}{\hbar^2 v_m}\int_{t_0}^{\tau_0} d\tau_1\frac{\alpha_1(\tau_1)}{\hbar}\eta^{(0)}(x_1,\tau_1) + \int_{t_0}^{t-\frac{x-x_1}{v_m}} d\tau_0\frac{\alpha_1(\tau_0)^2}{\hbar^2 v_m}\int_{t_0}^{\tau_0} d\tau_1\frac{\alpha_1(\tau_1)^2}{\hbar^2 v_m}\int_{t_0}^{\tau_1}\frac{\alpha_1(\tau_2)}{\hbar}\eta^{(0)}(x_1,\tau_2) + \cdots\right\}. \quad \text{(A10)}$$

Now the order of integrations in each term can be rearranged with the following identity:

$$\int_{t_0}^{A} d\tau_0 g(\tau_0) \int_{t_0}^{\tau_0} d\tau_1 f(\tau_1) = \int_{t_0}^{A} d\tau_1 f(\tau_1) \int_{\tau_1}^{A} d\tau_0 g(\tau_0) \xrightarrow{\tau_0 \leftrightarrow \tau_1} \int_{t_0}^{A} d\tau_0 f(\tau_0) \int_{\tau_0}^{A} d\tau_1 g(\tau_1). \tag{A11}$$

After summing infinite terms, one obtains

$$\eta^{(1)}(x,t) = \eta^{(0)}(x,t) - \Theta(x-x_1) \frac{\alpha_1(t-(x-x_1)/v_m)}{\hbar^2 v_m} \int_{t_0}^{t-\frac{x-x_1}{v_m}} d\tau_0\, \alpha_1(\tau_0)\, K_1\left(\tau_0, t - \frac{x-x_1}{v_m}\right) \eta^{(0)}(x_1,\tau_0). \tag{A12}$$

We note that this solution of $\eta^{(1)}(x,t)$ can be fully related by initial operators, $\eta(x,t_0)$.

To include the coupling at x_2 in Eq. (A7), we can use $\eta^{(1)}(x,t)$ as the incoming condition for Eq. (A7) at $x = x_2$ because of the chirality of the EOM. Therefore, the full solution of (A7) is given by

$$\eta(x,t) = \eta^{(1)}(x,t) - \Theta(x-x_2) \frac{\alpha_2\left(t - \frac{x-x_2}{v_m}\right)}{\hbar^2 v_m} \int_{t_0}^{t-\frac{x-x_2}{v_m}} d\tau_0\, \alpha_2(\tau_0)\, K_2\left(\tau_0, t - \frac{x-x_2}{v_m}\right) \eta^{(1)}(x_2,\tau_0). \tag{A13}$$

Again, the solution of $\eta(x,t)$ is expressed in terms of $\eta(x,t_0)$. Finally, the contribution of initial operators $\eta(x,t_0)$ to $\gamma_a(t)$, i.e., the second part (the integration part) of solutions in Eqs. (3.2), can be obtained by employing Eq. (A5) with the solution in Eq. (A13).

APPENDIX B: EDGE-INDUCED POLARIZATION

The goal of this appendix is to describe the phenomenon of edge-induced polarization, namely the nonzero expectation value $\langle i\gamma_1(t)\gamma_2(t)\rangle$ for two Majorana modes coupled to a chiral Majorana single edge [9]. Here we will focus on the situation where the coupling constants α_1 and α_2 are time independent and will consider the limit $\Delta x = x_2 - x_1 \to 0$ and $t \to \infty$. In this limit, we observe that the contributions of initial operators $\bar{\gamma}_a$ to Eqs. (3.2) decay exponentially and hence the only important contributions are those resulting from the coupling to the chiral edge state. Hence γ_a's can be approximated as

$$\begin{aligned} \gamma_1(t) &\sim -\alpha_1 \textstyle\int_{t_0}^{t} dt' K_1(t',t)\eta^{(0)}(x_1,t'), \\ \gamma_2(t) &\sim -\alpha_2 \textstyle\int_{t_0}^{t} dt' K_2(t',t)\eta^{(1)}(x_2,t'). \end{aligned} \tag{B1}$$

The qubit polarization is then formally expressed as

$$\langle i\gamma_1(t)\gamma_2(t)\rangle = i\frac{\alpha_1\alpha_2}{\hbar^2}\left\langle \int_{t_0}^{t} dt' K_1(t',t)\eta^{(0)}(x_1,t') \int_{t_0}^{t} dt'' K_2(t'',t)\left(\eta^{(0)}(x_2,t'') - \frac{\alpha_1^2}{\hbar^2 v_m}\int_{t_0}^{t''} d\tau_0 K_1(\tau_0,t'')\eta^{(0)}(x_1,\tau_0)\right)\right\rangle, \tag{B2}$$

where we have used Eq. (A12) with $\Delta x \to 0^+$ for $\eta^{(1)}(x_2,t')$. We observe that the polarization are induced through two mechanisms: (I) polarization due to direct entanglement of Majorana modes and edge state, i.e., the first part of Eq. (B2), and (II) polarization due to transfer quantum information of Majorana mode γ_1 to mode γ_2 through the edge, i.e., the second part of Eq. (B2).

Before we evaluate the magnitude of the induced polarization, we first observe that

$$K_a(t_i,t_f) = \exp\left[-\frac{\alpha_a^2}{2\hbar^2 v_m}(t_f - t_i)\right] \tag{B3}$$

because α_a is time independent. We will also need the following correlation function

$$\langle \eta^{(0)}(x,t)\eta^{(0)}(y,t')\rangle = \frac{1}{i\pi}\frac{1}{(x-y) - v_m(t'-t'')}. \tag{B4}$$

Let us first focus on the contribution from mechanism (I),

$$\langle i\gamma_1(t)\gamma_2(t)\rangle_{(I)} = i\frac{\alpha_1\alpha_2}{\hbar^2}\int_{t_0}^{t} dt' \int_{t_0}^{t} dt'' K_1(t',t)K_2(t'',t)\langle \eta^{(0)}(x_1,t')\eta^{(0)}(x_2,t'')\rangle. \tag{B5}$$

Using Eqs. (B3) and (B4) together with changes of variables $\tau' = t - t'$ and $\tau'' = t - t''$, we have

$$-\frac{\alpha_1\alpha_2}{\pi\hbar^2 v_m}\int_0^{\infty} d\tau' \int_0^{\infty} d\tau'' \frac{\exp\left[-\frac{\alpha_1^2}{2\hbar^2 v_m}\tau' - \frac{\alpha_2^2}{2\hbar^2 v_m}\tau''\right]}{\tau'' - \tau'}. \tag{B6}$$

Here we have taken $t - t_0 \to \infty$. With a further change of variable $T = (\tau' + \tau'')/2$ and $\Delta\tau = (\tau'' - \tau')/2$, the double integral can be carried out and gives

$$\langle i\gamma_1\gamma_2(t \to \infty)\rangle_{(I)} = \frac{2\alpha_1\alpha_2}{\pi\left(\alpha_2^2 + \alpha_1^2\right)} \ln\left(\frac{\alpha_2}{\alpha_1}\right)^2. \tag{B7}$$

Now we turn to evaluate the contribution from mechanism (II),

$$\langle i\gamma_1(t)\gamma_2(t)\rangle_{(II)} = -i\frac{\alpha_1^3\alpha_2}{\hbar^4 v_m}\int_{t_0}^{t} dt' K_1(t',t)\int_{t_0}^{t} dt'' K_2(t'',t)\int_{t_0}^{t''} d\tau_0 K_1(\tau_0,t'')\langle\eta^{(0)}(x_1,t')\eta^{(0)}(x_1,\tau_0)\rangle. \tag{B8}$$

Exchanging the order of integral over t'' and τ_0 and using Eq. (A11) and explicitly integrating out t'', we obtain

$$\frac{2\alpha_1^3\alpha_2}{\pi\hbar^2 v_m\left(\alpha_2^2 - \alpha_1^2\right)}\int_{t_0}^{t} dt' e^{-\frac{\alpha_1^2}{2\hbar^2 v_m}(t-t')}\int_{t_0}^{t} d\tau_0 \frac{e^{\frac{\alpha_1^2}{2\hbar^2 v_m}(\tau_0 - t)} - e^{\frac{\alpha_2^2}{2\hbar^2 v_m}(\tau_0 - t)}}{t' - \tau_0}. \tag{B9}$$

By performing changes of variables $\tau' = t - t'$ and $\tau'' = t - \tau_0$ and taking $t - t_0 \to \infty$, we then have

$$\frac{2\alpha_1^3\alpha_2}{\pi\hbar^2 v_m\left(\alpha_2^2 - \alpha_1^2\right)}\int_0^{\infty} d\tau' d\tau'' e^{-\frac{\alpha_1^2\tau'}{2\hbar^2 v_m}} \frac{e^{-\frac{\alpha_1^2\tau''}{2\hbar^2 v_m}} - e^{-\frac{\alpha_2^2\tau''}{2\hbar^2 v_m}}}{\tau'' - \tau}. \tag{B10}$$

This integral is similar to that in Eq. (B6). Hence, with similar procedure, we can show that

$$\langle i\gamma_1\gamma_2(t \to \infty)\rangle_{(II)} = \frac{4\alpha_1^3\alpha_2}{\pi\left(\alpha_2^2 - \alpha_1^2\right)\left(\alpha_2^2 - \alpha_1^2\right)} \ln\left(\frac{\alpha_2}{\alpha_1}\right)^2. \tag{B11}$$

By adding two parts of contributions, the total polarization when two Majorana modes are coupled to the edge is given by

$$\langle i\gamma_1\gamma_2(t \to \infty)\rangle = \frac{2\alpha_1\alpha_2}{\pi\left(\alpha_2^2 - \alpha_1^2\right)} \ln\left(\frac{\alpha_2}{\alpha_1}\right)^2. \tag{B12}$$

This result is consistent with what was found in Ref. [9] and has its peak value $2/\pi$ for $\alpha_1/\alpha_2 = 1$.

APPENDIX C: UNEQUAL VELOCITIES

If the two edge states propagate with different velocities, the approach taken in the main text, Secs. II and III, is no longer valid. One cannot reduce the problem to that of a single edge state. Instead, we can investigate directly the Green's function that enters the calculation of W_{2E} in Eq. (3.6). Starting with the Hamiltonian of the two edges, we have

$$H_e = \int dx\left\{-i\frac{\hbar}{4}[v_L\eta^L(x)\partial_x\eta^L(x) + v_R\eta^R(x)\partial_x\eta^R(x)] + im(x)\eta^L(x)\eta^R(x)\right\}. \tag{C1}$$

This can be rewritten in terms of Pauli matrices:

$$H_e = \int dx\left\{\begin{pmatrix}\eta^L\\ \eta^R\end{pmatrix}^{\dagger}\left[-i\frac{\hbar}{4}(\overline{v}\mathbf{1} + \delta v\sigma^z)\partial_x + m(x)\sigma^y\right]\begin{pmatrix}\eta^L\\ \eta^R\end{pmatrix}\right\}, \tag{C2}$$

where we define $\delta v = (v_L - v_R)/2$ and $\overline{v} = (v_L + v_R)/2$. The equations of motion for the Green function are

$$\left[\partial_t + (\overline{v}\mathbf{1} + \delta v\sigma^z)\partial_x - i\frac{m(x)}{\hbar}\sigma^y\right]\begin{pmatrix}G_{\eta^L}(x - x', t - t')\\ G_{\eta^R}(x - x', t - t')\end{pmatrix} = \mathbf{1}\delta(x - x')\delta(t - t'). \tag{C3}$$

Here, x' and t' are the source space and time. When $m(x)$ has no spatial dependence, the Green's function is formally resolved in Fourier space as

$$G(x - x', t - t') = -i\int\frac{dk}{2\pi}\int\frac{d\omega}{2\pi}\frac{(\overline{v}k - \omega) - \delta vk\sigma^z + (m/\hbar)\sigma^y}{(\overline{v}k - \omega)^2 - (\delta vk)^2 - (m/\hbar)^2}e^{ik(x-x') - i\omega(t-t')}. \tag{C4}$$

By integrating over the frequency domain and choosing the pole that gives the retarded Green's function, we obtain

$$\begin{aligned} G(x - x', t - t') = \Theta(t - t')\int\frac{dk}{2\pi}\frac{e^{ik(x-x')}}{2}\Bigg[&(e^{-i\omega_+(t-t')} + e^{-i\omega_-(t-t')}) + \frac{\hbar\delta vk\sigma^z}{\sqrt{m^2 + \hbar^2k^2\delta v^2}}(e^{-i\omega_+(t-t')} - e^{-i\omega_-(t-t')})\\ &+ \frac{m\sigma^y}{\sqrt{m^2 + \hbar^2k^2\delta v^2}}(e^{-i\omega_-(t-t')} - e^{-i\omega_+(t-t')})\Bigg], \end{aligned} \tag{C5}$$

with $\omega_\pm = \overline{v}k \pm \sqrt{(m/\hbar)^2 + k^2\delta v^2}$. In the limit $\delta v \to 0$, the 2×2 Green's function becomes

$$G(x-x',t-t') = \Theta(t-t')\delta((x-x')-\overline{v}(t-t'))\Big(\cos\Big(\frac{m}{\hbar}(t-t')\Big)\mathbf{1} + i\ \sin\Big(\frac{m}{\hbar}(t-t')\Big)\sigma_y\Big), \tag{C6}$$

after taking the k integration. As an alternative way, this Green's function will lead to results obtained in Sec. III B.

Because the term that mixes the two edges plays an important role for constructing W_{2E} in Eq. (3.6), we shall focus on the off-diagonal σ_y term, $G_y(x-x',t-t')$. The role this function plays becomes clear when we consider how to modify the result for the all-important W function from Eq. (3.5). The way our answer is modified when the velocities are different is

$$W(t_0,t,\Delta x) = -\int_{t_0}^{t} dt_1 \int_{t_1}^{t} dt_2 \frac{\alpha_2(t_2)\alpha_1(t_1)}{\hbar^2 v_m} K_2(t',t_2)K_1(t_0,t_1)G_y(\Delta x, t_2-t_1), \tag{C7}$$

and $G_y(\Delta x,t_2-t_1)$ reduces to a $\sin\Delta\theta\cdot\delta(t_2-t_1-\Delta x/v)$ in the equal-velocity case, with $\Delta\theta$ defined in Eq. (3.8).

Let us next approximate $G_y(\Delta x,t_2-t_1)$. To allow information transferring between the two edges, we must have $\frac{m\Delta x}{\hbar\overline{v}} \sim 1$ and hence $\frac{\hbar k\overline{v}}{m} \sim 1$. In the limit $\delta v \ll \overline{v}$, we can confine ourselves to the case of $\hbar k\delta v \ll m$. Thus we can expand the expression in Eq. (C5) to the second order in δv and obtain a Gaussian integral

$$\begin{aligned} G_y(x-x',t-t') &\approx \Theta(t-t')\int \frac{dk}{2\pi}\frac{\sigma^y}{2} e^{ik[(x-x')-\overline{v}(t-t')]}\Big(e^{-\frac{1}{2}(\frac{\hbar\delta v k}{m})^2 + i(\frac{m}{\hbar}+\frac{\hbar(k\delta v)^2}{2m})(t-t')} - e^{-\frac{1}{2}(\frac{\hbar\delta v k}{m})^2 - i(\frac{m}{\hbar}+\frac{\hbar(k\delta v)^2}{2m})(t-t')}\Big) \\ &= i\sigma^y\Theta(t-t')\frac{m}{\sqrt{2\pi}\hbar\delta v}\mathrm{Im}\left[\frac{e^{-\frac{1}{2}\left(\frac{m}{\hbar\delta v}\right)^2\frac{((x-x')-\overline{v}(t-t'))^2}{1-im(t-t')/\hbar} + im(t-t')/\hbar}}{\sqrt{1-i\,m(t-t')/\hbar}}\right]. \end{aligned} \tag{C8}$$

$G_y(\Delta x,t_2-t_1)$ has a time width of about $\delta t \sim \frac{\hbar\delta v}{\overline{v}m}$ around $(x-x')-\overline{v}(t-t')=0$. Hence the higher $\frac{mx}{\hbar\overline{v}}$ is, the more oscillatory the function will be as a function of time at the second Majorana site. Observe that Eq. (C8) reduces to the result in Eq. (C6) for $\frac{\hbar\delta v}{m} \to 0$. As a result, we expect that the effect of the velocity difference becomes negligible when $\frac{\hbar\delta v}{m} \ll \Delta x$. In the limit of our consideration, this condition is in general satisfied. Indeed, carrying out the integral in Eq. (C8) approximately yields a simple suppression term of $e^{(-\delta v/v)^2}$ relative to the results in Fig. 2.

[1] J. M. Leinaas and J. Myrheim, Nuovo Cimento B **37**, 1 (1977).
[2] F. Wilczek, Phys. Rev. Lett. **48**, 1144 (1982).
[3] F. Wilczek, Phys. Rev. Lett. **49**, 957 (1982).
[4] D. Arovas, J. R. Schrieffer, and F. Wilczek, Phys. Rev. Lett. **53**, 722 (1984).
[5] G. Moore and N. Read, Nucl. Phys. B **360**, 362 (1991).
[6] C. Nayak and F. Wilczek, Nucl. Phys. B **479**, 529 (1996).
[7] C. Nayak, S. H. Simon, A. Stern, M. Freedman, and S. Das Sarma, Rev. Mod. Phys. **80**, 1083 (2008).
[8] A. Y. Kitaev, Ann. Phys. (NY) **303**, 2 (2003).
[9] D. J. Clarke and K. Shtengel, New J. Phys. **13**, 055005 (2011).
[10] F. Hassler, A. R. Akhmerov, C.-Y. Hou, and C. W. J. Beenakker, New J. Phys. **12**, 125002 (2010).
[11] P. Bonderson and R. M. Lutchyn, Phys. Rev. Lett. **106**, 130505 (2011).
[12] F. Hassler, A. R. Akhmerov, and C. W. J. Beenakker, New J. Phys. **13**, 095004 (2011).
[13] D. Pekker, C.-Y. Hou, V. E. Manucharyan, and E. Demler, Phys. Rev. Lett. **111**, 107007 (2013).
[14] A. A. Kovalev, A. De, and K. Shtengel, Phys. Rev. Lett. **112**, 106402 (2014).
[15] G. Volovik, Pis'ma Zh. Eksp. Teor. Fiz. **70**, 601 (1999) [JETP Lett. **70**, 609 (1999)].
[16] N. Read and D. Green, Phys. Rev. B **61**, 10267 (2000).
[17] D. A. Ivanov, Phys. Rev. Lett. **86**, 268 (2001).
[18] J. Alicea, Rep. Prog. Phys. **75**, 076501 (2012).
[19] C. W. J. Beenakker, Annu. Rev. Condens. Matter Phys. **4**, 113 (2013).
[20] V. Mourik, K. Zuo, S. M. Frolov, S. R. Plissard, E. P. A. M. Bakkers, and L. P. Kouwenhoven, Science **336**, 1003 (2012).
[21] M. T. Deng, C. L. Yu, G. Y. Huang, M. Larsson, P. Caroff, and H. Q. Xu, Nano Lett. **12**, 6414 (2012).
[22] A. Das, Y. Ronen, Y. Most, Y. Oreg, M. Heiblum, and H. Shtrikman, Nat. Phys. **8**, 887 (2012).
[23] L. P. Rokhinson, X. Liu, and J. K. Furdyna, Nat. Phys. **8**, 795 (2012).
[24] S. Nadj-Perge, I. K. Drozdov, J. Li, H. Chen, S. Jeon, J. Seo, A. H. MacDonald, B. A. Bernevig, and A. Yazdani, Science **346**, 602 (2014).
[25] A. Y. Kitaev, Phys. Usp. **44**, 131 (2001).
[26] R. M. Lutchyn, J. D. Sau, and S. Das Sarma, Phys. Rev. Lett. **105**, 077001 (2010).
[27] Y. Oreg, G. Refael, and F. von Oppen, Phys. Rev. Lett. **105**, 177002 (2010).
[28] S. Nadj-Perge, I. K. Drozdov, B. A. Bernevig, and A. Yazdani, Phys. Rev. B **88**, 020407 (2013).
[29] S. Bravyi, Phys. Rev. A **73**, 042313 (2006).
[30] H.-J. Kwon, K. Sengupta, and V. Yakovenko, Eur. Phys. J. B **37**, 349 (2004).
[31] I. Serban, B. Béri, A. R. Akhmerov, and C. W. J. Beenakker, Phys. Rev. Lett. **104**, 147001 (2010).
[32] N. Y. Yao, C. R. Laumann, A. V. Gorshkov, H. Weimer, L. Jiang, J. I. Cirac, P. Zoller, and M. D. Lukin, Nat. Commun. **4**, 1585 (2011).
[33] B. Rosenow, B. I. Halperin, S. H. Simon, and A. Stern, Phys. Rev. Lett. **100**, 226803 (2008).
[34] B. Rosenow, B. I. Halperin, S. H. Simon, and A. Stern, Phys. Rev. B **80**, 155305 (2009).
[35] E. Grosfeld and A. Stern, Proc. Natl. Acad. Sci. USA **108**, 11810 (2011).
[36] X. G. Wen, Phys. Rev. B **43**, 11025 (1991).